Hindawi
Journal of Nanotechnology
Volume 2019, Article ID 3424915, 11 pages
https://doi.org/10.1155/2019/3424915

Research Article

Growth of MWCNTs on Plasma Ion-Bombarded Thin Gold Films and Their Enhancements of Ammonia-Sensing Properties Using Inkjet Printing

Udomdej Pakdee[1] **and Ananya Thaibunnak**[2]

[1]*Division of Physics, Faculty of Science and Technology, Rajamangala University of Technology Krungthep, Bangkok 10120, Thailand*
[2]*Division of Printing Technology, Faculty of Science and Technology, Rajamangala University of Technology Krungthep, Bangkok 10120, Thailand*

Correspondence should be addressed to Udomdej Pakdee; udomdej.p@mail.rmutk.ac.th

Received 19 January 2019; Revised 11 April 2019; Accepted 23 April 2019; Published 2 June 2019

Academic Editor: Enkeleda Dervishi

Multiwalled carbon nanotubes (MWCNTs) have been synthesized on thin gold (Au) films using thermal chemical vapor deposition (CVD). The films were evolved to catalytic Au nanoparticles (Au NPs) by plasma argon (Ar) ion bombardment with a direct current (DC) power of 216 W. The characteristics of the MWCNTs grown on Au catalysts are strongly dependent on the growth temperature in thermal CVD process. The MWCNTs were then purified by oxidation (550°C) and acid treatments (3 : 1 H_2SO_4/HNO_3). After purifying the MWCNTs, they were dispersed in deionized water (DI water) under continuous sonication. The MWCNT solution was then ultrasonically dissolved in a conducting polymer mixture of poly(3,4-ethylenedioxythiophene):poly(styrenesulfonate) (PEDOT:PSS) to prepare for an electronic ink. The ink was deposited onto the flexible and transparent plastic substrates such as polyethylene terephthalate (PET) with fabricated silver interdigitated electrode using two methods such as drop-casting and inkjet printing to compare in the detection of ammonia (NH_3) and other volatile organic compounds (VOCs) at room temperature. Based on the results, the gas response, sensitivity, and selectivity properties of MWCNT-PEDOT:PSS gas sensor for NH_3 detection are significantly enhanced by using inkjet printing technique. The sensing mechanism of fabricated gas sensor exposed to NH_3 has been also proposed based on the swelling behaviour of polymer due to the diffusion of NH_3 molecules into the polymer matrix. For the MWCNTs, they were mentioned as the conductive pathways for the enhancement of gas-sensing signals.

1. Introduction

Carbon nanotubes (CNTs) and their composites have attracted increasing attention in various applications for several years [1–5]. Many techniques have been presented to synthesize the multiwalled carbon nanotubes (MWCNTs) and single-walled carbon nanotubes (SWCNTs) [6–9]. Chemical vapor deposition (CVD) is one of the most popular techniques for growing the CNTs. In this technique, metal catalyst particles or islands were presented as an important factor for growing the MWCNTs [10]. Recently, there have been extensive reports to demonstrate the growth of CNTs by using gold nanoparticles (Au NPs) as catalysts [11–14]. The catalyst behaviour of Au NPs can be presented when its particle size is reduced into nanoscale caused by size effects [14]. Because of the resistance to oxidation and good electric conductivity, the Au catalysts would be an ideal selection for the fabrication of CNT-based devices. The evolution of thin Au films to nanoparticles using thermal annealing and plasma ion bombardment was successfully reported for growing the CNTs [13]. For gas-sensing applications, the CNTs can be promoted as a good material due to its excellent properties such as high specific surface area, good electric conductivity, and high carrier mobility [15, 16]. The publications involving the gas-sensing devices have been focused on the high sensitivity and good selectivity at room temperature [16–19]. The CNTs decorated with some metal nanoparticles as a sensing film were reported to improve the

gas-sensing properties [20–23]. Furthermore, nitrogen doping and functionalization of CNTs with some organic compounds have been also presented to enhance the gas response to ammonia (NH_3) and other volatile organic compounds (VOCs) [24, 25]. Direct charge transfer process and reducing reaction between NH_3 and chemisorbed oxygen were presented as dominant processes for NH_3-sensing mechanism [21, 25].

In this work, the MWCNTs were grown on plasma ion-bombarded thin Au films by thermal CVD. The effects of growth temperature on the MWCNT morphologies and their crystalline qualities were demonstrated. After growing the MWCNTs, they were then prepared to a sensing film in form of an electronic ink by using purified MWCNT dispersion in poly(3,4-ethylenedioxythiophene):poly(styrenesulfonate) (PEDOT:PSS) conducting polymer. The novel method in deposition of sensing film onto the plastic substrates with fabricated silver interdigitated electrodes by using inkjet printing technique for the enhancement of NH_3-sensing properties at room temperature was also evaluated. In addition, the sensing mechanism of fabricated NH_3 gas sensor has been proposed based on the swelling of the PEDOT:PSS polymer matrix together with the enhancement of sensing signals by MWCNTs.

2. Materials and Methods

2.1. Preparation of Substrate. Copper foils (~50 μm thick) purchased from Brastech Company were used as substrates for growing the all MWCNTs. Firstly, the Cu substrates were mechanically polished with silicon carbide grinding papers (grit 3000). Then, they were cut into $3 \times 3\,cm^2$ size samples and subsequently cleaned in acetone followed by methanol for 15 min and dried with nitrogen (N_2). The topographies of Cu substrates before and after polishing the surface are shown in Figures 1(a) and 1(b), respectively. Aluminum oxide (Al_2O_3) films with a thickness of 45 nm as buffer layers were first deposited onto the Cu substrates by a homemade reactive direct current (DC) magnetron sputtering. Thin gold films with a thickness of 10 nm were then deposited on Al_2O_3 films by using a commercial DC sputter coater (Scancoat Six; BOC Edwards). The thicknesses of buffer and catalyst films were chosen from the repeatedly previous work of us as a suitable thickness for the optimum result. The details of deposited conditions for the films kept in this study are shown in Table 1.

2.2. Formation of Catalytic Au NPs by Plasma Ion Bombardment. The Au/Al_2O_3 films deposited on Cu foils as substrates were ultrasonically cleaned with methanol and dried with N_2. For modifying the substrate, the sample was fixed with two screws on Cu target as a sample holder within a reactor chamber. Schematic illustration and photograph of chamber for plasma ion bombardment are shown in Figures 2(a) and 2(b), respectively. The chamber was evacuated to obtain a base pressure of 5×10^{-5} mbar by using an operation of a rotary pump and a diffusion pump. After obtaining the base pressure, Ar was introduced into the chamber with a flow rate of 5 sccm. The target was supplied with a constant power of 216 W (0.4 A and 540 V) by a DC power supply in Ar plasma for 5 min to achieve the formation of catalytic Au NPs on the substrate.

2.3. Growth of MWCNT by Thermal CVD. Again, the modified substrates were ultrasonically cleaned with methanol and dried with N_2 before inserting them into a horizontal quartz chamber of a home-built thermal CVD system. The details of this system were reported by the previous work of the first author [26]. The chamber was evacuated to the pressure of 10^{-2} mbar with a rotary pump (Alcatel, 2012). Argon was fed into the chamber with a flow rate of 200 sccm while heating up the chamber to the growth temperatures of 880°C. The mixture of hydrogen (H_2) and acetylene (C_2H_2) gases was fed into the chamber with the flow rates of 100 sccm and 60 sccm, respectively. All gases were introduced through three flow meter controllers (Cole-Parmer, TW03227-12). After the thermal CVD process, the MWCNTs were grown, and they were cooled down under Ar atmosphere with a flow rate of 50 sccm until the temperature inside the chamber was nearly room temperature. The process was carefully repeated for the growth temperatures of 900 and 950°C, respectively.

2.4. Characterizations. The topography of Cu substrates was examined by an atomic force microscope (AFM, AR MFP-3D). After growing the MWCNTs, the samples were characterized in their morphologies by using a Quanta 450 FEI scanning electron microscope (SEM) working at 30 kV and 10 μA. The as-grown MWCNTs were removed from the substrate by a sonication in a dimethyl sulfoxide (DMSO) compound and dropped on a gold grid for analysis under high-resolution transmission electron microscope (HRTEM, Hitachi HT 7700) operated with energy dispersive X-ray spectroscopy (EDS). The crystalline qualities of MWCNTs grown on different growth temperature were identified by a Fourier-transform Raman spectrometer (FT-Raman, PerkinElmer Spectrum GX).

2.5. Fabrication of Gas Sensor and Gas-Sensing Measurements. After growing the MWCNTs, the samples were purified by oxidation treatment at 550°C for 30 min followed by the acid-treated process using a mixture of sulfuric acid and nitric acid (3 : 1 H_2SO_4/HNO_3) under continuous sonication for 2 h. The purified MWCNTs were rinsed several times with distilled water and dried at 60°C in an oven. For preparing the precursor inks, 0.5 g of purified MWCNT powder was dispersed in 80 ml of deionized water (DI water) under continuous sonication for 2 h. The MWCNT solution was then ultrasonically dissolved in a polymer mixture of PEDOT:PSS with a weight ratio of 10% MWCNT solution to 90% PEDOT:PSS for 45 min. The inks were deposited onto the plastic substrates such as polyethylene terephthalate (PET) by two methods for comparison in their gas-sensing properties at room temperature. One was a simple method, i.e., drop-casting, and the other was an applied method,

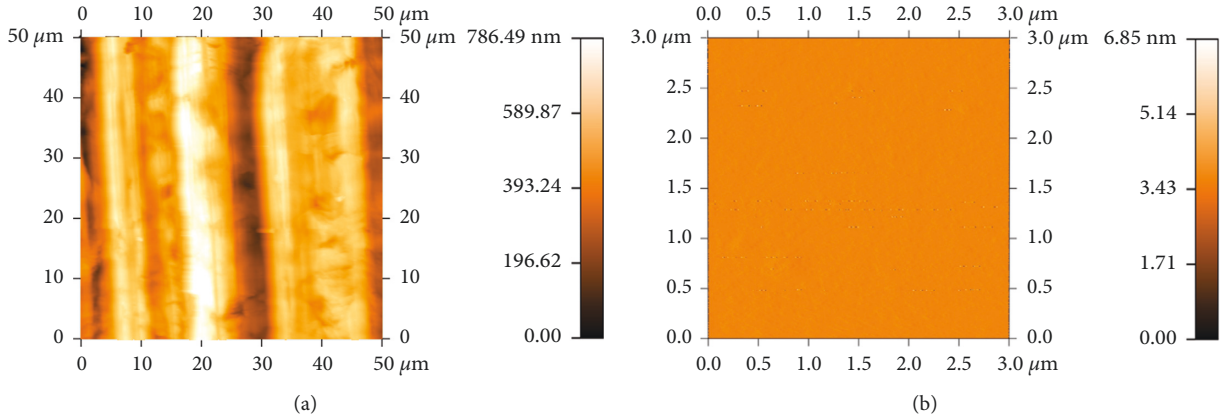

Figure 1: AFM topographical images of (a) as-received Cu foil and (b) polished Cu foil.

Table 1: Sputtered conditions for deposition of Al_2O_3 and Au films.

Parameters	Al_2O_3 film	Au film
Base pressure (mbar)	5×10^{-5}	5×10^{-3}
Working pressure (mbar)	3×10^{-3}	1×10^{-1}
Substrate temperature (°C)	R.T	R.T
Distance between the target and the substrate (cm)	10	5
Ar flow rate (sccm)	5	5
O_2 flow rate (sccm)	1	—
DC power (W)	216	20
Sputtering time (s)	60	30

i.e., inkjet printing. For the drop-casted method, the ink with a volume of 20 μl was dropped onto the substrate by using a micropipette. For the inkjet printing technique, an ordinary inkjet office printer (HP deskjet ink 1112) was applied for printing the sensing films over the substrates. The ordinary ink in the printer was eliminated from a cartridge. The empty cartridge was carefully refilled with the 20 μl MWCNT-PEDOT:PSS conducting ink. It should be noted that the MWCNT content has been limited to 10 wt.% due to the problem of clogged nozzles in the printer-head. Then, the 20 μl ink was inkjet-printed on the substrate with 5 printed layers. A flow-through system was designed to measure the gas response of our gas sensors. The details of gas measurement system were explained by a previous work of our groups [18]. The test gas and dry air flow rates were carefully controlled by two flow meters. Small volume of dry air was introduced to test solution for supplying its vapor into the test chamber. The various volatile organic compounds (VOCs) such as NH_3, methanol, acetone, and dimethylformamide (DMF) in a form of solution were chosen to study the selectivity property of fabricated gas sensors. Cylindrical quartz was used as a test chamber. The chamber was connected with the flow-through system and a design voltage divider circuit. A 10 V applied voltage as a power source was supplied to the circuit for measuring the sensor resistances. The data were monitored every second using a LabVIEW software and a NI USB DAQ 6008 device displayed with a laptop. All observations were operated at room temperature (26 ± 2°C) in dry air.

3. Results and Discussion

Figure 3 shows the AFM topographical images of Au/Al_2O_3 films after Ar ion bombarding and annealing processes. The mean roughness of the film as shown in Figure 3(a) is approximately 18.6 nm. The roughness was maybe due to the formation of Au grains according to the condition upon energy supply from Ar ion-bombardment. A 10 nm Au film with an Al_2O_3 buffer layer was chosen to understand the morphology of the catalyst during the CVD process. The sample was replicated in all CVD conditions without the carbon source. As shown in Figure 3(b), the surface roughness of the film is approximately 4.5 nm. It is clearly seen that the surface roughness of Au catalyst film after annealing process is lower than the film before annealing. This result could be discussed due to the filling of catalyst particles on the buffer layer after annealing process [27]. The filling mechanism of catalyst particles on the buffer layer can be explained using Figure 4. During the CVD annealing, the high temperature is a major cause for the rough surface of the underneath catalyst layer (i.e., buffer layer). Because the thickness of Au film is approximately 10 nm, it does not cover the surface of the Al_2O_3 buffer layer. However, it full fills the collapse area of buffer film surface. Therefore, the lower roughness of substrate as shown in Figure 3(b) could be attributed to the roughness of buffer layer after the CVD annealing.

Figure 5 shows the MWCNTs grown on Ar ion-bombarded substrates using Au NPs as catalysts with different growth temperatures of 880, 900, and 950°C. It is seen that the MWCNTs were grown in the temperature range of 900–950°C (Figures 5(b)-5(c)). However, they were not observed on the substrate at the growth temperature of 880°C (Figure 5(a)). This is due to the fact that higher growth temperatures lead to high exothermic reaction from C_2H_2 to MWCNTs. The high energy for carbon decomposition can easily heat the Au catalysts to the suitable temperature for MWCNT growth. Therefore, the growth temperature must be high enough to allow for the formation of the MWCNTs on the Au catalysts. To confirm the catalyst compositions, the MWCNTs were removed on their substrates using sonication in DMSO solvent and dropped them on a gold

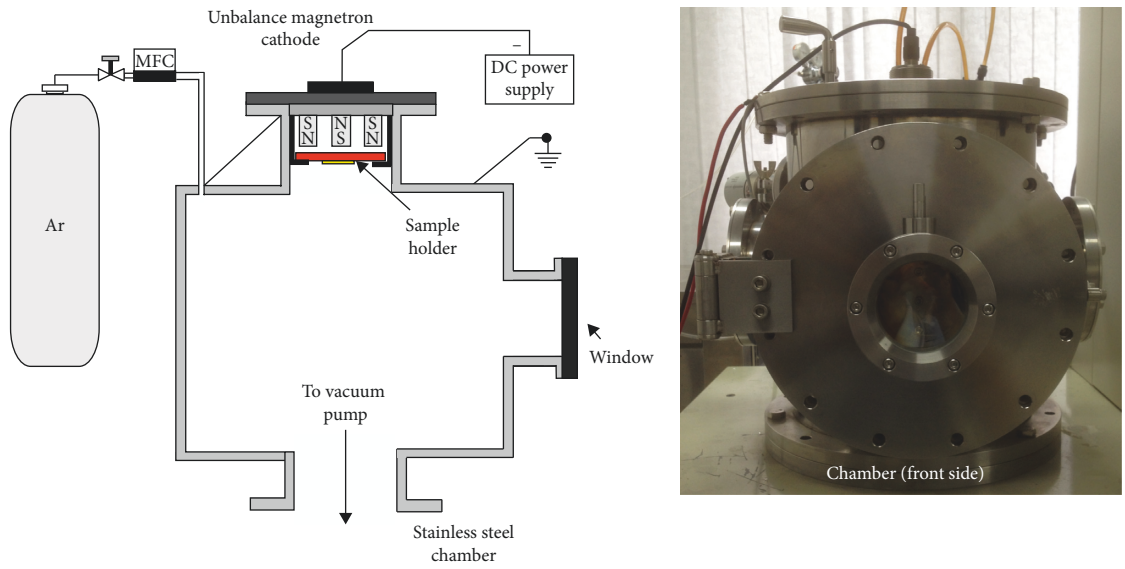

Figure 2: (a) Schematic illustration and (b) photograph of reactor chamber for plasma ion bombardment.

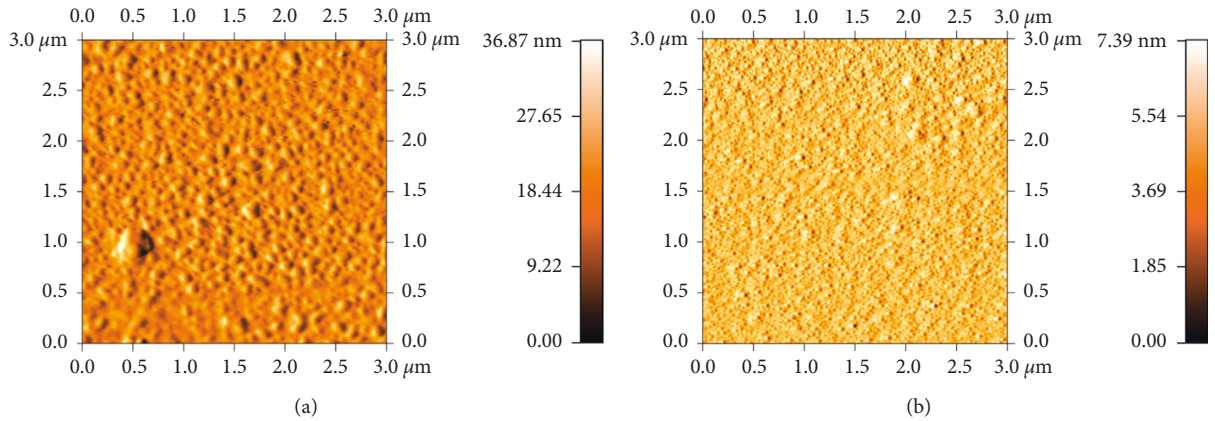

Figure 3: AFM topographical images of sputtered Au/Al_2O_3 films deposited on polished Cu foil (a) after bombarding with Ar ion and (b) after annealing processes.

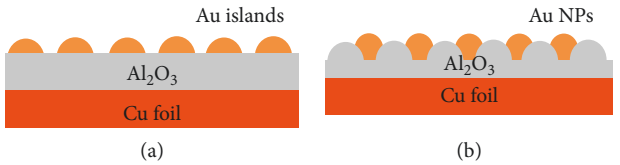

Figure 4: Schematic illustration of filling mechanism for Au films deposited onto the Al_2O_3/Cu foils (a) after bombarding with Ar ion and (b) after annealing processes.

TEM grid. The EDS spectrum of a catalyst particle under a TEM grid is shown in Figure 5(d). The spectrum on the catalyst showed the signals of C and Au and no signal for Al or other metals. Therefore, an Au nanoparticle as shown with inset image of HRTEM in Figure 5(d) can be confirmed to be a catalyst for MWCNT growth even though some signals of Au may be obtained from the TEM grid.

The crystalline qualities of MWCNTs grown on substrates have been identified using intensity ratio of D to G bands (I_D/I_G) of Raman spectrum [28, 29]. The D and G bands are defined as the amorphous carbonaceous impurities or defects with sp^3 carbon bonds (~1350 cm^{-1}) and graphitic nature of carbon with sp^2 carbon bonds (~1580 cm^{-1}), respectively [28]. Figure 6 shows the Raman spectra of MWCNTs grown on substrates at temperatures of 900°C and 950°C. It is seen that the I_D/I_G ratios for the MWCNTs grown on substrate at 900°C and 950°C are found to be 1.08 and 0.84, respectively. It was discussed that the adjacent Au nanoparticles could be combined and formed into a larger particle at high temperature (950°C). The formation of amorphous carbon structures on the large catalyst was identified by using the diffusion model for CNT formation. The model predicts that if the size of catalyst is larger than the diffusion length of carbon, CNT growth is poor [28]. As can be seen in Figure 3(a), some big Au particles were formed beside the small nanoparticles. They

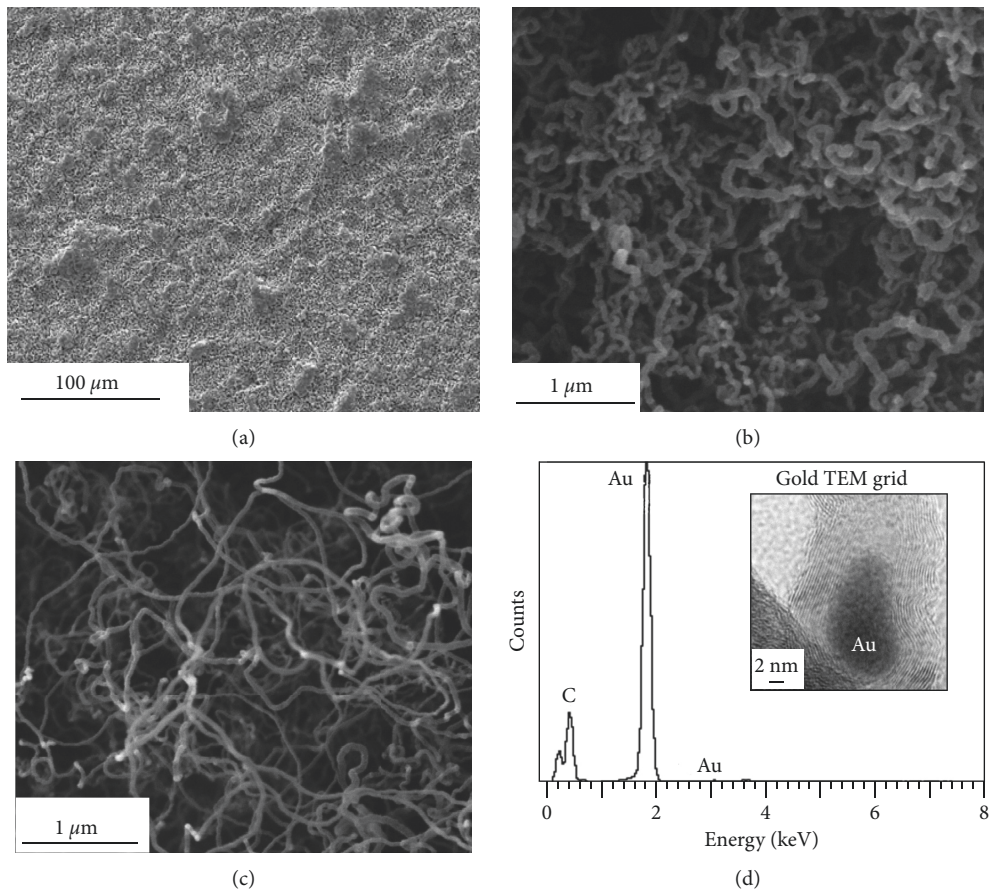

Figure 5: SEM images of MWCNTs grown using different growth temperatures with Au nanoparticles as catalysts: (a) 880°C, (b) 900°C, and (c) 950°C. (d) EDS signals of MWCNT with an Au catalyst particle under TEM.

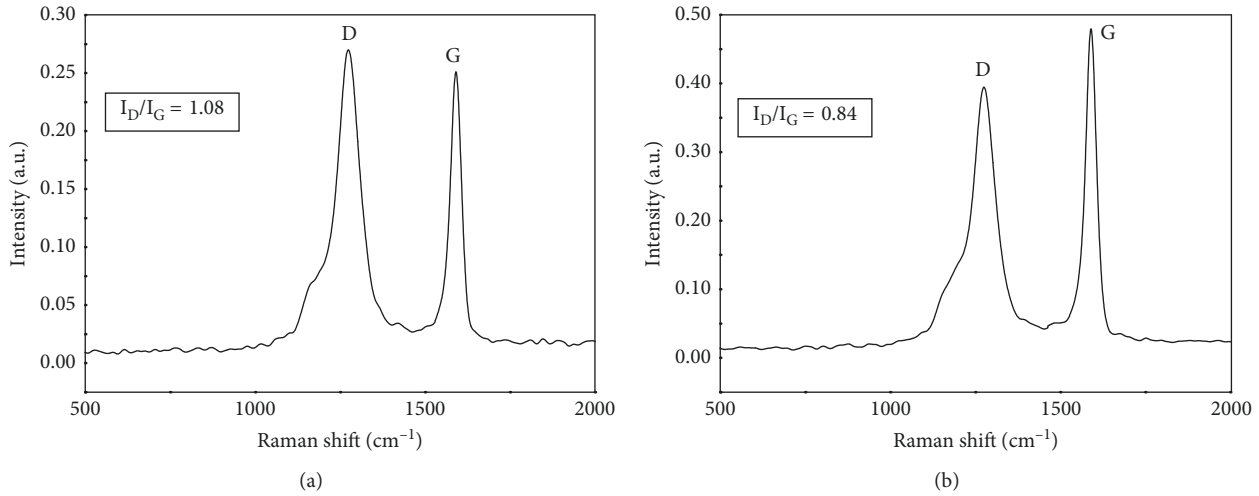

Figure 6: Raman spectra of MWCNTs grown using different growth temperatures of (a) 900°C and (b) 950°C.

cause the formation of amorphous carbon structures. This may be the source why the ratio of D to G-band intensity of the grown MWCNTs at 950°C is still quite large. The optimum result such as the MWCNTs grown on Ar ion-bombarded thin Au film at growth temperature of 950°C was further more investigated.

The poor dispersion of MWCNTs within aqueous solution is still a main problem for the preparation of sensing ink in gas sensor applications. Therefore, surface modification and functionalization of MWCNTs with some organic compounds are required for their enhancements of solubility and compatibility properties. In this work, the

MWCNTs were purified by oxidation treatment followed by the acid-treated process using a mixture of sulfuric acid and nitric acid (3 : 1 H_2SO_4/HNO_3) under continuous sonication. These processes have been claimed in the removal of carbonaceous impurities and attachment of carboxylic (COOH) organic compounds on the CNT surface [30].

To understand the effect of purified process on the dispersion quality of MWCNTs, 0.5 g of purified MWCNTs was immersed in 80 ml DI water under continuous sonication for 2 h. Figure 7(a) shows photographs of purified MWCNT solution after storage in 1 day and the selfsame solution after storage in 30 days. It can be observed that the solution is stable during storage in 30 days. This is indicative of the high dispersion quality for purified MWCNTs with excellent sensing performance. The solution was then dissolved in a conducting polymer mixture of PEDOT:PSS to prepare for an electronic ink. The ink was deposited onto the flexible and transparent plastic substrates with fabricated silver interdigitated electrode using two methods including drop-casting and inkjet printing. The schematic diagram of the structure for fabricated gas sensor is shown in Figure 7(b).

Figure 8 shows the SEM images of MWCNT-PEDOT:PSS sensing films on silver interdigitated electrode deposited by drop-casting and inkjet printing. The morphologies of sensing film obtained from drop-casting method are shown in Figures 8(a) and 8(b). Due to the high surface tension of PEDOT:PSS, the droplets of sensing film with different sizes tend to form in a low compress and poor coverage on the substrate surface. On the other hand, the MWCNT-PEDOT:PSS sensing film obtained from inkjet printing gave the best compress in terms of coverage and density as shown in Figures 8(c) and 8(d). It can be seen in the insert image of Figure 8(d) that the MWCNTs are randomly imbedded in the matrix of PEDOT:PSS polymer.

The performance of our fabricated gas sensors was evaluated using gas response and sensitivity and selectivity properties. The gas response was defined by equation (1). For the sensitivity, it is the slope of linear graph in the relation of gas response versus gas concentration. The selectivity was defined as a comparative gas response between different VOC test gases:

$$S(\%) = \frac{R_{\text{gas}} - R_{\text{air}}}{R_{\text{air}}} \times 100, \quad (1)$$

where R_{gas} and R_{air} are the resistances of the gas sensor in test gas and dry air, respectively.

Figure 9 shows the resistance changes of gas sensors prepared by drop-casting and inkjet printing with a function of NH_3 concentrations (Figure 9(a)) and the comparative gas response of sensor exposed to various VOCs with a fixed concentration of 1000 ppm (Figure 9(b)). For the resistance change in response to NH_3, it is seen that the sensor obtained from inkjet printing condition has much higher baseline resistance than the sensor from drop-casting. It was also discussed that the filling of oxygen vacancies on MWCNT surface obtained from a heating element in an inkjet printer could lead to the increase in baseline resistance of gas sensor. In both cases, the changes of resistance are proportional to decreasing concentration of NH_3 gas from 1000 to 100 ppm.

In case of drop-casted condition, the gas responses of MWCNT-PEDOT:PSS gas sensor exposed to NH_3 in the concentrations of 100, 200, 500, and 1000 ppm are found to be 0.2, 0.3, 0.8, and 2.1%, respectively. In the same NH_3 concentrations, the gas responses of MWCNT-PEDOT:PSS gas sensor obtained from inkjet-printed condition are also found to be 8.5, 23.3, 40.7, and 73.7%, respectively. The selectivity of MWCNT-PEDOT:PSS gas sensors was further investigated by using different VOC vapors including methanol, acetone, and DMF as the test gases as shown in Figure 9(b). It is seen that the sensor obtained from drop-casting shows the very low responses and low selectivity to all test gases. On the other hand, the sensor obtained from inkjet printing exhibits high response to NH_3 (~74%), while its response to other VOCs are low (≤10%).

It is well known that both PEDOT:PSS and MWCNTs are p-type semiconductors [31, 32]. In this work, the fabricated MWCNT-PEDOT:PSS gas sensors also behave as a p-type semiconductor since the resistances of drop-casted and inkjet-printed gas sensors increase when NH_3 reducing gases are absorbed on their sensing films (Figure 9(a)). In addition, the gas response of inkjet-printed MWCNT-PEDOT:PSS gas sensor was further investigated with an oxidizing gas (i.e., nitrogen dioxide (NO_2)). A tank of NO_2 (99.5% purity) was connected with the flow-through system as a source of target gas. During the NO_2-sensing measurement, the resistances of gas sensor were recorded every second using a LabVIEW software program and a NI USB DAQ 6008 device. It has been found in Figure 10 that the sensor shows no noticeable response to NO_2 at room temperature. However, the sensor exhibits a slight decrease of resistance upon exposure to NO_2, corresponding to the p-type semiconductor gas sensor towards an oxidizing gas [33]. This result can be discussed that the hole charge carriers could be higher than the charge transfer due to integration between two p-type semiconductor materials. This leads to the very low response of our gas sensor for an electron acceptor as NO_2. Based on the gas-sensing results, the inkjet-printed MWCNT-PEDOT:PSS gas sensor is performed to show the highest response and highest selectivity to NH_3 at room temperature. Although the sensor cannot perfectly recover to baseline resistance, the property of the sensor in response to NH_3 at high concentrations is much higher compared to some other works [17–19].

To understand the effects of MWCNT content on the gas-sensing performance of fabricated gas sensor, the bare PEDOT:PSS and the PEDOT:PSS with the low content of MWCNTs were further more investigated. Although the MWCNT contents are up to 2, 5, and 8 wt.%, the gas responses of the sensors are similar to the case of bare PEDOT:PSS polymer. This is due to the lack of MWCNTs within the precursor inks. The MWCNTs were mentioned as the conductive pathways for the enhancement of sensing signals.

For the carbon-based gas sensor in literature data, the working range of baseline resistance in response to NH_3 was indicated to be in the order of kΩ [34, 35]. The amount of MWCNTs within the precursor inks has an effect on the baseline line or initial resistance of the sensors. The initial resistance of MWCNT gas sensor decreased when the

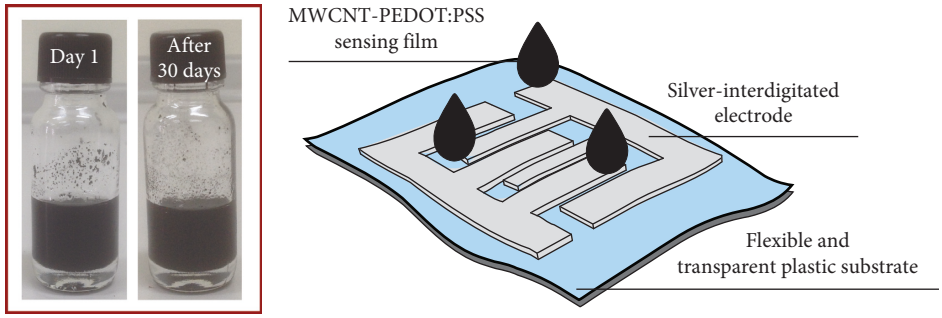

Figure 7: (a) Photographs of purified MWCNTs immersed in DI water after storage in 1 day and 30 days. (b) Schematic diagram of a fabricated gas sensor.

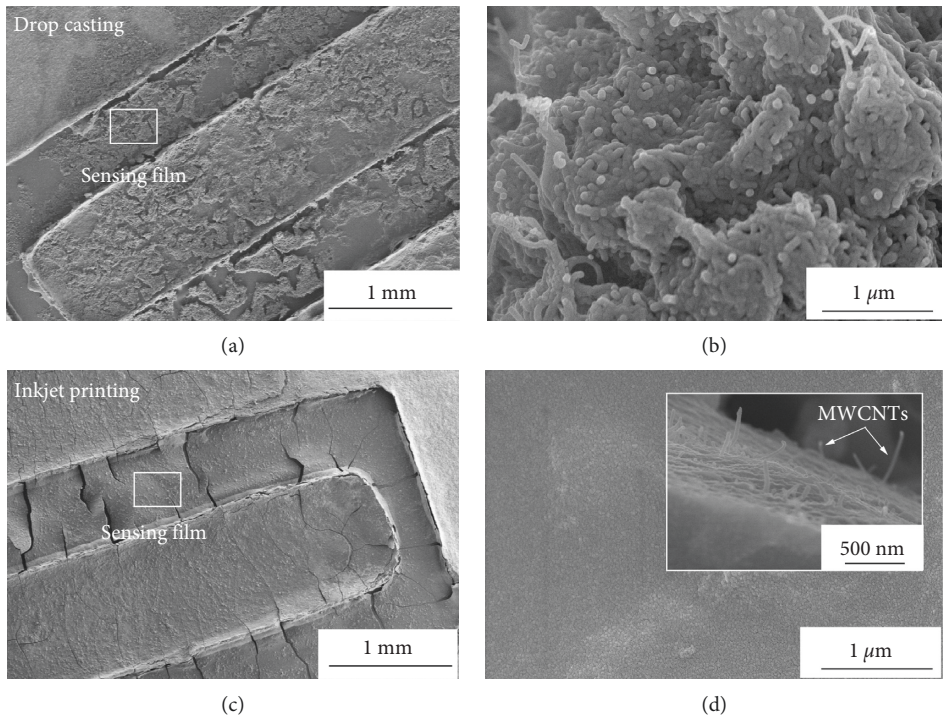

Figure 8: SEM images of MWCNT-PEDOT:PSS sensing film on silver interdigitated electrode using (a-b) drop-casting and (c-d) inkjet printing.

MWCNT content of sensor was increased. In this work, the initial resistances of inkjet-printed and drop-casted MWCNT gas sensors with a weight ratio of 10% MWCNTs to 90% PEDOT:PSS were found to be 1.80 and 0.96 kΩ, respectively. These values fall within the working range of initial resistance for fabricated gas sensor in response to NH_3 (i.e., around kΩ). This is the main reason why the weight ratio of 10% MWCNTs to 90% PEDOT:PSS was considered to be the optimization of MWCNT concentration.

There have been some papers reporting that the PEDOT:PSS polymer can be used as a sensing film for NH_3 detection [19, 36, 37]. Figure 11 shows the resistance changes of the inkjet-printed gas sensors preparing the sensing film with bare PEDOT:PSS (Figure 11(a)) and MWCNT-PEDOT:PSS (Figure 11(b)). Two sensors were further exposed to a single pulse of 1000 ppm NH_3 at room temperature. It is observed that the sensors present the increments of resistance upon exposure to NH_3 vapors before they almost recover to their baseline lines in dry air. After calculating the gas response, the response values of inkjet-printed PEDOT:PSS and inkjet-printed MWCNT-PEDOT:PSS gas sensors are found to be ~4.0% and ~74.0%, respectively. Thus, the bare PEDOT:PSS gas sensor is still able to respond to NH_3 and its response is substantially enhanced after MWCNT integration.

Figure 12 shows a graph of gas response as a function of NH_3 concentration for the sensors prepared by drop-casting and inkjet printing. It is seen that the gas response increased with increasing NH_3 concentration. Furthermore, it is also found that the sensor obtained from inkjet printing technique showed higher NH_3 gas response than the sensor obtained from drop-casting in every NH_3 concentration. This is because of the homogeneous gain effect when the

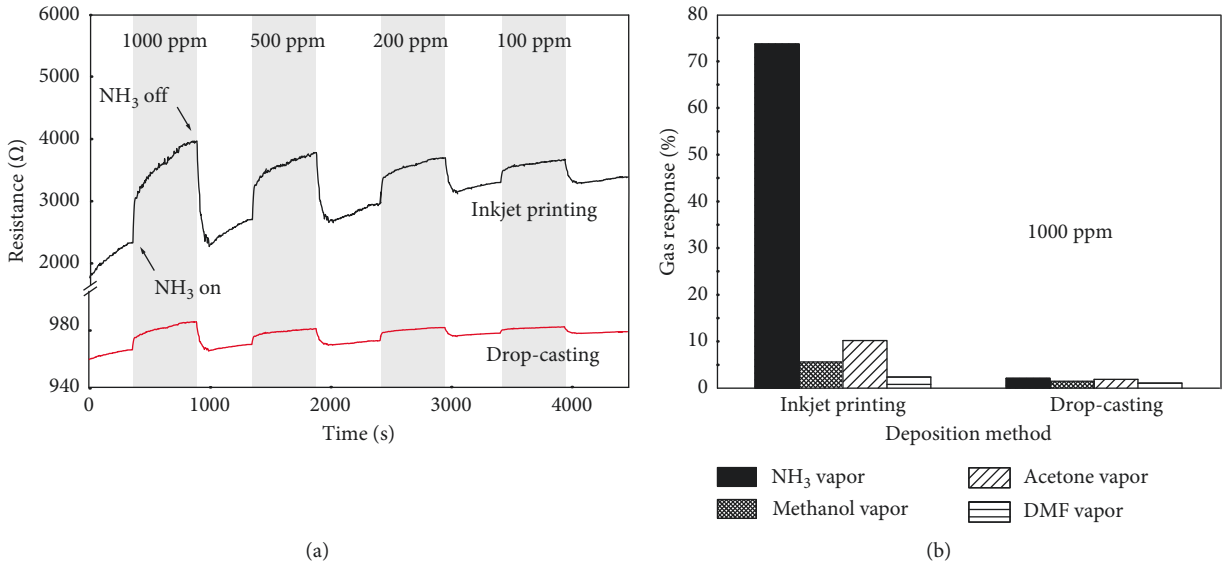

Figure 9: (a) Resistance changes of the fabricated gas sensors prepared by drop-casting and inkjet printing exposed to NH_3 with various concentrations. (b) Gas response of sensor exposed to various VOCs with a fixed concentration of 1000 ppm.

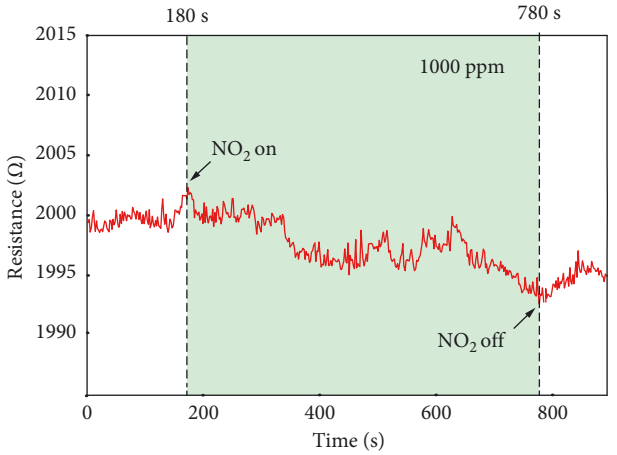

Figure 10: Resistance change of inkjet-printed MWCNT-PEDOT:PSS gas sensor exposed to 1000 ppm NO_2 at room temperature.

sensing film is inkjet-printed on the substrate unlike in the case of drop-casted deposition. This effect was previously explained in the enhancement of carrier conductive pathways [38, 39]. The sensitivities of drop-casted and inkjet-printed MWCNT-PEDOT:PSS gas sensors calculated from the linear regression line are found to be 0.002 and 0.069 ppm^{-1}, respectively. Therefore, the inkjet-printed MWCNT-PEDOT:PSS gas sensor has significantly higher sensitivity than the drop-casted MWCNT-PEDOT:PSS gas sensor after exposure to NH_3 in the concentration range of 100 ppm to 1000 ppm.

The schematic illustration of conductive pathways in electron transports for inkjet-printed MWCNT-PEDOT:PSS and drop-casted MWCNT-PEDOT:PSS networks is shown in Figures 13(a) and 13(b), respectively. Because of the excellent compress and good coverage of inkjet-printed MWCNT-PEDOT:PSS networks, a series of highly conductive pathways for electron transports was formed between the silver

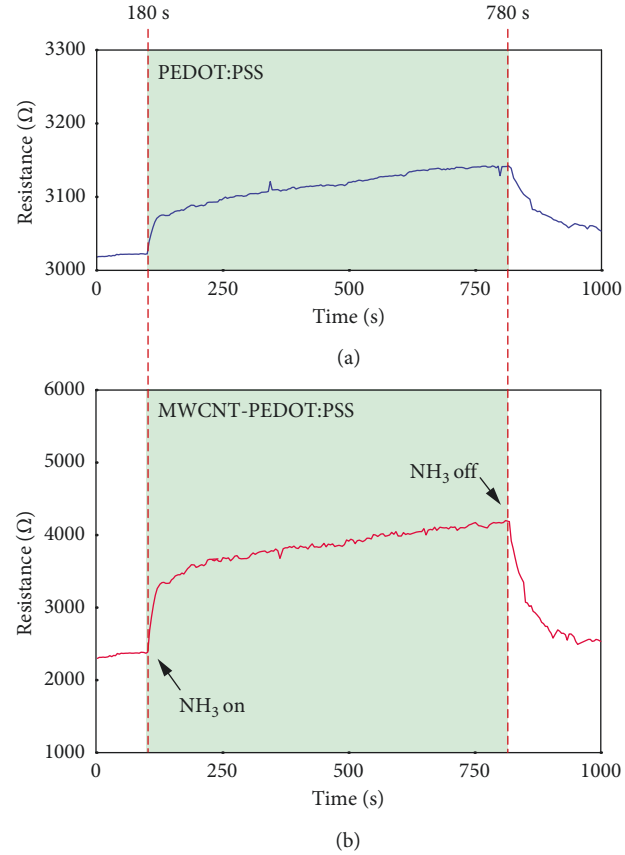

Figure 11: Resistance changes of the gas sensors prepared by inkjet printing exposed to 1000 ppm NH_3 with (a) bare PEDOT:PSS and (b) MWCNT-PEDOT:PSS as sensing films.

contracts. On the other hand, due to the high surface tension of PEDOT:PSS, the mismatch between the drop-casted MWCNT-PEDOT:PSS junctions creates the low conductive pathways for electron transports. This cause leads to the low

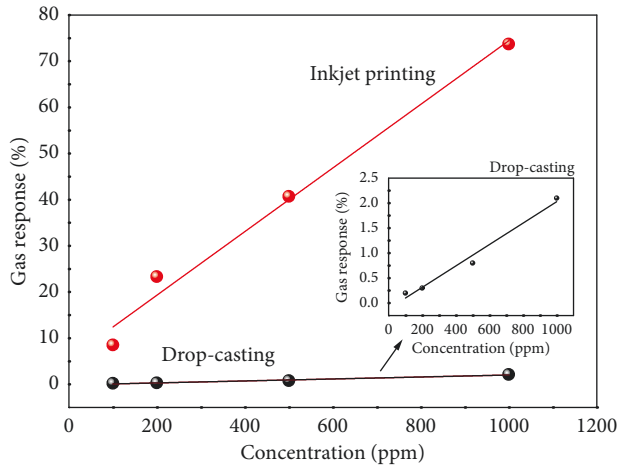

FIGURE 12: Gas responses of fabricated gas sensors prepared by drop-casting and inkjet printing as a function of NH_3 concentration at room temperature.

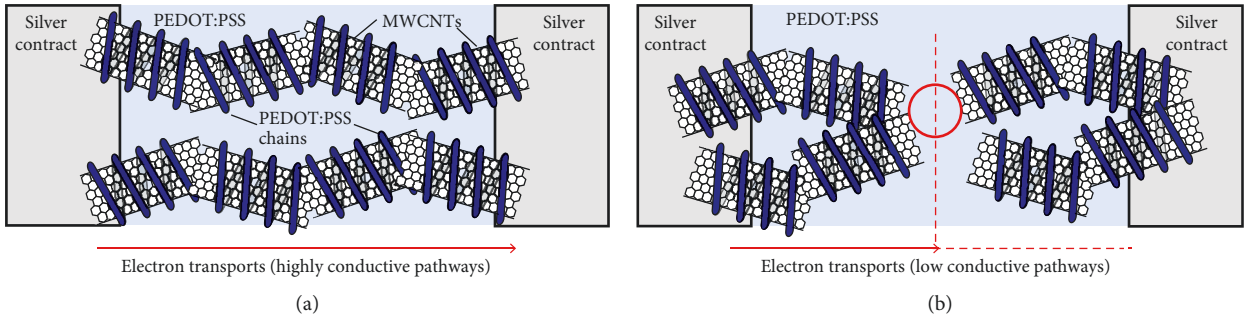

FIGURE 13: Schematic illustration of conductive pathways in electron transports for (a) inkjet-printed MWCNT-PEDOT:PSS networks and (b) drop-casted MWCNT-PEDOT:PSS networks.

signals for the NH_3 response of drop-casted MWCNT-PEDOT:PSS gas sensor.

The response time was defined as the time of resistance change for the sensor after a gas-sensing cycle. The response time of sensors from all experiments was measured for ~10 min. However, the resistance of all fabricated sensors does not perfectly return to its baseline resistance, although the NH_3 flow is stopped. Therefore, the recovery time of all fabricated sensors cannot be indicated due to the fact that the NH_3 molecules will diffuse slowly throughout the polymer chains by dry air purging at room temperature. The sensing mechanism of the PEDOT:PSS polymer-based gas sensor can be mentioned by using a swelling process [40, 41]. The possible sensing mechanism of the sensor in this study was discussed based on the fact that the MWCNTs embedded into PEDOT:PSS matrix act as conductive pathways. A PSS chain in PEDOT:PSS polymer interacts with PEDOT chains over its length. There is a very short distance of interchain for PEDOT to allow for the presentation of electron hopping process. The swelling process leads to the disruption of the conductive pathways in the sensing film. After the diffusion of NH_3 molecules into the PEDOT:PSS matrix, the interchain distance of PEDOT was increased because of the swelling process. Therefore, the electron hopping process could be able to more difficult. This cause leads to a significant increase in the resistance of the MWCNT-PEDOT:PSS gas sensor upon exposure to the NH_3 vapors.

The NH_3-sensing measurements were further repeated every week for 30 days. It has been found that the inkjet-printed MWCNT-PEDOT:PSS gas sensor presents the good stability with only ~5% of letdown from its initial response under room temperature storage. Baseline drift is a vital performance parameter of gas sensor. It appears when the sensor response has changed over time. In this study, the baseline resistances of sensors are higher after detecting a high NH_3 concentration and shift upward from the initial baseline resistance after 4 sensing cycles at room temperature (Figure 9(a)). This is due to the fact that the NH_3 molecules under a high concentration are not desorbed completely on the sensing film at room temperature. All the parameters of our sensors may not be the highest performance achieved nowadays. However, the authors try to present the fact that the deposition of sensing film by inkjet printing technique may be a good selection in combination with other factors for the powerful gas-sensing performance at room temperature.

4. Conclusions

The MWCNTs have been successfully grown on plasma ion-bombarded thin gold films using thermal CVD process.

The optimum temperature for the growth of effective MWCNTs on the films is 950°C. The purified MWCNT solution was mixed together with a conducting polymer of PEDOT:PSS for preparing an electronic ink. The inkjet printing of gas-sensing ink from an ordinary inkjet office printer has been presented as a good method for enhancement of NH_3 gas-sensing properties at room temperature. The inkjet-printed MWCNT-PEDOT:PSS gas sensor presents the p-type semiconductor behaviour under NH_3 and NO_2 gases. The enhanced sensing properties of NH_3 gas sensor were attributed to homogeneous gain effect of sensing films to improve the MWCNT conductive pathways for the electron transports. The dominant sensing mechanism of fabricated NH_3 gas sensor has been further presented based on the swelling of the polymer due to the diffusion of NH_3 molecules into the chains of polymer matrix. This finding can be beneficial for application in printable or wearable NH_3 gas-sensing technology.

Data Availability

The data used to support the findings of this study are available from the corresponding author upon request.

Conflicts of Interest

The authors declare that there are no conflicts of interest regarding the publication of this paper.

Acknowledgments

This work was funded by the Research and Development Institute, Rajamangala University of Technology Krungthep, Thailand. The authors are thankful to Mr. Gun Chaloeipote, one of the Ph.D. students from Department of Physics, Faculty of Science, Kasetsart University, Thailand, for fruitful cooperation.

References

[1] S. Yoon, S. Lee, S. Kim, K.-W. Park, D. Cho, and Y. Jeong, "Carbon nanotube film anodes for flexible lithium ion batteries," *Journal of Power Sources*, vol. 279, pp. 495–501, 2015.

[2] R. M. Silva, A. C. Bastos, F. J. Oliveira et al., "Catalyst-free growth of carbon nanotube arrays directly on Inconel® substrates for electrochemical carbon-based electrodes," *Journal of Materials Chemistry A*, vol. 3, no. 34, pp. 17804–17810, 2015.

[3] S. K. Ujjain, P. Ahuja, R. Bhatia, and P. Attri, "Printable multi-walled carbon nanotubes thin film for high performance all solid state flexible supercapacitors," *Materials Research Bulletin*, vol. 83, pp. 167–171, 2016.

[4] Q. Zeng, H. Tian, J. Jiang, X. Ji, D. Gao, and C. Wang, "High-purity helical carbon nanotubes with enhanced electrochemical properties for supercapacitors," *RSC Advances*, vol. 7, no. 12, pp. 7375–7381, 2017.

[5] K. S. Lee, M. J. Shin, C. W. Park, and J.-D. Kim, "Simple and direct synthesis of ZnO decorated multi-walled carbon nanotube for supercapacitor electrodes," *Colloids and Surfaces A: Physicochemical and Engineering Aspects*, vol. 538, pp. 23–27, 2018.

[6] Y. Su, Z. Yang, H. Wei, E. S.-W. Kong, and Y. Zhang, "Synthesis of single-walled carbon nanotubes with selective diameter distributions using DC arc discharge under CO mixed atmosphere," *Applied Surface Science*, vol. 257, no. 7, pp. 3123–3127, 2011.

[7] L. Lascialfari, P. Marsili, S. Caporali et al., "Carbon nanotubes/laser ablation gold nanoparticles composites," *Thin Solid Films*, vol. 569, pp. 93–99, 2014.

[8] C. Zhuo, X. Wang, W. Nowak, and Y. A. Levendis, "Oxidative heat treatment of 316L stainless steel for effective catalytic growth of carbon nanotubes," *Applied Surface Science*, vol. 313, pp. 227–236, 2014.

[9] J. Zhao, L. Wei, Z. Yang, and Y. Zhang, "Continuous and low-cost synthesis of high-quality multi-walled carbon nanotubes by arc discharge in air," *Physica E: Low-dimensional Systems and Nanostructures*, vol. 44, no. 7-8, pp. 1639–1643, 2012.

[10] C. J. Lee, J. Park, and J. A. Yu, "Catalyst effect on carbon nanotubes synthesized by thermal chemical vapor deposition," *Chemical Physics Letters*, vol. 360, no. 3-4, pp. 250–255, 2002.

[11] M. Yamada, M.-A. Kawana, and M. Miyake, "Synthesis and diameter control of multi-walled carbon nanotubes over gold nanoparticle catalysts," *Applied Catalysis A: General*, vol. 302, no. 2, pp. 201–207, 2006.

[12] C. Luo, L. Liu, K. Jiang, L. Zhang, Q. Li, and S. Fan, "Growth mechanism of Y-junctions and related carbon nanotube junctions synthesized by Au-catalyzed chemical vapor deposition," *Carbon*, vol. 46, no. 3, pp. 440–444, 2008.

[13] S.-H. Lee, E.-H. Kwak, H.-S. Kim, S.-W. Lee, and G.-H. Jeong, "Evolution of gold thin films to nanoparticles using plasma ion bombardment and their use as a catalyst for carbon nanotube growth," *Thin Solid Films*, vol. 547, pp. 188–192, 2013.

[14] Y. Homma, "Gold nanoparticles as the catalyst of single-walled carbon nanotube synthesis," *Catalysts*, vol. 4, no. 1, pp. 38–48, 2014.

[15] X. Zhang, X. Wu, B. Yang, and H. Xiao, "Enhancement of gas sensing characteristics of multiwalled carbon nanotubes by CF_4 plasma treatment for SF_6 decomposition component detection," *Journal of Nanomaterials*, vol. 2015, Article ID 171545, 9 pages, 2015.

[16] N. Janudin, N. Abdullah, W. M. Z. W. Yunus et al., "Effect of functionalized carbon nanotubes in the detection of benzene at room temperature," *Journal of Nanotechnology*, vol. 2018, Article ID 2107898, 7 pages, 2018.

[17] L. Nguyen, P. Phan, H. Duong, C. Nguyen, and L. Nguyen, "Enhancement of NH_3 gas sensitivity at room temperature by carbon nanotube-based sensor coated with Co nanoparticles," *Sensors*, vol. 13, no. 2, pp. 1754–1762, 2013.

[18] U. Pakdee, P. Phunudom, S. Nantakarat et al., "Room temperature gas sensor based on helical carbon coils," *Key Engineering Materials*, vol. 798, pp. 105–110, 2019.

[19] C. Wongchoosuk, P. Jangtawee, P. Lokavee, S. Udomrat, P. Sudkeaw, and T. Kerdcharoen, "Novel flexible NH_3 gas sensor prepared by ink-jet printing technique," *Advanced Materials Research*, vol. 506, pp. 39–42, 2012.

[20] M. Han, D. Jung, and G. S. Lee, "Palladium-nanoparticle-coated carbon nanotube gas sensor," *Chemical Physics Letters*, vol. 610-611, pp. 261–266, 2014.

[21] K. Lee, V. Scardaci, H.-Y. Kim et al., "Highly sensitive, transparent, and flexible gas sensors based on gold nanoparticle decorated carbon nanotubes," *Sensors and Actuators B: Chemical*, vol. 188, pp. 571–575, 2013.

[22] F. Rigoni, G. Drera, S. Pagliara, A. Goldoni, and L. Sangaletti, "High sensitivity, moisture selective, ammonia gas sensors

based on single-walled carbon nanotubes functionalized with indium tin oxide nanoparticles," *Carbon*, vol. 80, pp. 356–363, 2014.

[23] S.-W. Choi, J. Kim, and Y. T. Byun, "Highly sensitive and selective NO_2 detection by Pt nanoparticles-decorated single-walled carbon nanotubes and the underlying sensing mechanism," *Sensors and Actuators B: Chemical*, vol. 238, pp. 1032–1042, 2017.

[24] E. Gracia-Espino, B. Rebollo-Plata, H. Martínez-Gutiérrez et al., "Temperature dependence of sensors based on silver-decorated nitrogen-doped multiwalled carbon nanotubes," *Journal of Sensors*, vol. 2016, Article ID 4319498, 10 pages, 2016.

[25] S. Sharma, K. Sengupta, and S. S. Islam, "Deposition of pristine and functionalized MWCNTs in alumina matrix by sol-gel technique and investigation of their ammonia sensing properties," *Nanomaterials and Nanotechnology*, vol. 2, p. 4, 2012.

[26] U. Pakdee, S. Chiangga, S. Suwannatus, and P. Limsuwan, "Growth of MWCNTs on flexible stainless steels without additional catalysts," *Journal of Nanomaterials*, vol. 2017, Article ID 5672728, 11 pages, 2017.

[27] J. S. Kim, Y.-W. Jang, and I.-T. Im, "Growth of vertical carbon nanotubes according to the Al_2O_3 buffer layer preparation," *Journal of Industrial and Engineering Chemistry*, vol. 19, no. 5, pp. 1501–1506, 2013.

[28] G. Atthipalli, R. Epur, P. N. Kumta et al., "The effect of temperature on the growth of carbon nanotubes on copper foil using a nickel thin film as catalyst," *Thin Solid Films*, vol. 519, no. 16, pp. 5371–5375, 2011.

[29] G. Atthipalli, H. Wang, and J. L. Gray, "Catalyst-assisted vertical growth of carbon nanotubes on Inconel coated commercial copper foil substrates versus sputtered copper films," *Applied Surface Science*, vol. 273, pp. 515–519, 2013.

[30] V. T. Le, C. L. Ngo, Q. T. Le, T. T. Ngo, D. N. Nguyen, and M. T. Vu, "Surface modification and functionalization of carbon nanotube with some organic compounds," *Advances in Natural Sciences: Nanoscience and Nanotechnology*, vol. 4, no. 3, article 035017, 2013.

[31] C. Wongchoosuk, A. Wisitsoraat, D. Phokharatkul, A. Tuantranont, and T. Kerdcharoen, "Multi-walled carbon nanotube-doped tungsten oxide thin films for hydrogen gas sensing," *Sensors*, vol. 10, no. 8, pp. 7705–7715, 2010.

[32] Y. Lin, L. Huang, L. Chen et al., "Fully gravure-printed NO_2 gas sensor on a polyimide foil using WO_3-PEDOT:PSS nanocomposites and Ag electrodes," *Sensors and Actuators B: Chemical*, vol. 216, pp. 176–183, 2015.

[33] G. F. Fine, L. M. Cavanagh, A. Afonja, and R. Binions, "Metal oxide semi-conductor gas sensors in environmental monitoring," *Sensors*, vol. 10, no. 6, pp. 5469–5502, 2010.

[34] H. Lee, G. Shaker, K. Naishadham et al., "Carbon nanotube loaded antenna-based ammonia gas sensor," *IEEE Transactions on Microwave Theory and Techniques*, vol. 59, no. 10, pp. 2665–2673, 2011.

[35] O. Monereo, S. Claramunt, M. Martínez de Marigorta et al., "Flexible sensor based on carbon nanofibers with multifunctional sensing features," *Talanta*, vol. 107, pp. 239–247, 2013.

[36] N. Tang, Y. Jiang, H. Qu, and X. Duan, "Conductive polymer nanowire gas sensor fabricated by nanoscale soft lithography," *Nanotechnology*, vol. 28, no. 48, article 485301, 2017.

[37] S. Li, Y. Li, S. Chen et al., "Improved sensitivity of inkjet-printed PEDOT:PSS ammonia sensor with "Nonideal" morphology," *IEEE Sensors Letters*, vol. 2, no. 1, pp. 1–4, 2018.

[38] Y. H. Kim, C. Sachse, M. L. Machala, C. May, L. Müller-Meskamp, and K. Leo, "Highly conductive PEDOT:PSS electrode with optimized solvent and thermal post-treatment for ITO-free organic solar cells," *Advanced Functional Materials*, vol. 21, no. 6, pp. 1076–1081, 2011.

[39] A. Benchirouf, S. Palaniyappan, R. Ramalindame et al., "Electrical properties of multi-walled carbon nanotubes/PEDOT:PSS nanocomposites thin films under temperature and humidity effects," *Sensors and Actuators B: Chemical*, vol. 224, pp. 344–350, 2016.

[40] U. Latif and F. L. Dickert, "Graphene hybrid materials in gas sensing applications," *Sensors*, vol. 15, no. 12, pp. 30504–30524, 2015.

[41] L. Biessmann, L. P. Kreuzer, T. Widmann, N. Hohn, J.-F. Moulin, and P. Müller-Buschbaum, "Monitoring the swelling behavior of PEDOT:PSS electrodes under high humidity conditions," *ASC Applied Materials & Interfaces*, vol. 10, no. 11, pp. 9865–9872, 2018.